

# **Kinematic Processing Analysis of Carrier Phase based Precise Point Positioning**

**Xiaobing SHEN and Dr. Yang GAO, Canada**

**Key words:** Precise point positioning (PPP), ionosphere-free, precise GPS data, kinematics processing.

## **ABSTRACT**

This paper presents processing results of applying a new precise point positioning method at a kinematic mode. Analysis is conducted with respect to the positioning accuracy and convergence performance. The results have indicated an average positioning accuracy of 12 cm RMS vertically and less than 10 cm horizontally. An average of 2 hours is usually needed for the float position solution to converge to an accuracy of a few centimetres which points out the importance for the development of ambiguity resolution method for PPP processing.

## **CONTACT**

Mr. Xiaobing Shen and Dr. Yang Gao  
Department of Geomatics Engineering  
The University of Calgary  
2500 University Drive NW  
Calgary, Alberta  
CANADA T2N 1N4  
Tel. + 1 403 220 8150  
Fax + 1 403 284 1980  
E-mail: shenx@ucalgary.ca, gao@geomatics.ucalgary.ca

# Kinematic Processing Analysis of Carrier Phase based Precise Point Positioning

Xiaobing SHEN and Dr. Yang GAO, Canada

## INTRODUCTION

Different from the traditional carrier phase differential positioning technique that requires access to observations from one or more reference stations with known coordinates, Precise Point Positioning (PPP) involves only a single receiver, therefore, it is easy to deploy and cost-effective. Using precise satellite orbit and clock products from organizations contributing to the International GPS Service (IGS) including Natural Resources Canada (NRCAN), PPP has the potential to provide decimeter to centimeter position accuracy in stand-alone kinematic and static modes on a global scale [3][6]. As precise GPS orbit and clock products continue to improve in precision and timeliness and real-time phase-based wide-area/global ionospheric correction becomes available, PPP for real-time dm to cm positioning and navigation will become possible in the near future.

Previous PPP processing methods were mostly based on the traditional ionosphere-free combinations and the ambiguities are estimated in float values. It usually takes about 30 minutes for the float ambiguity unknowns to be converged in a static processing mode, so they are not suitable for the real-time fast-static and kinematic applications. A further improvement at a stand-alone mode requires the development of ambiguity resolution algorithms. In [1], a new observation system has been proposed which allows the exploitation of the integer characteristics of the carrier phase ambiguities. Numerical results have been presented there with respect to PPP processing at a static mode.

This paper presents some numerical results for PPP processing at a kinematic mode. The analysis includes the performance of the ambiguity convergence and the kinematic positioning accuracy after the ambiguity parameters are converged. The paper is organized as follows. Section 2 briefly outlines the mathematical model that has been developed for the new PPP processing method. PPP processing procedures are described in Section 3. Kinematic processing results and analysis are presented in Section 4 followed by the concluding remarks in Section 5.

## NEW OBSERVATION MODEL FOR PPP PROCESSING

With a dual-frequency GPS receiver, the code and phase measurements on  $L_i$  ( $i=1, 2$ ) between a GPS receiver and a GPS satellite can be described by the following equations [5]:

$$P(L_i) = \rho + c(dt - dT) + d_{orb} + d_{trop} + d_{ion/L_i} + d_{mult/P(L_i)} + \varepsilon(P(L_i)) \quad (1)$$

$$\begin{aligned} \Phi(L_i) = & \rho + c(dt - dT) + d_{orb} + d_{trop} - d_{ion/L_i} + \lambda_i N_i + \lambda_i (\phi_r(t_0, L_i) - \phi_s(t_0, L_i)) \\ & + d_{mult/\Phi(L_i)} + \varepsilon(\Phi(L_i)) \end{aligned} \quad (2)$$

where

$P(Li)$	is the measured pseudorange on Li (m);
$\Phi(Li)$	is the measured carrier phase on Li (m);
$\rho$	is the true geometric range (m);
$c$	is the speed of light (m/s);
$dt$	is the satellite clock error (s);
$dT$	is the receiver clock error (s);
$d_{orb}$	is the satellite orbit error (m);
$d_{trop}$	is the tropospheric delay (m);
$d_{ion/Li}$	is the ionospheric delay on Li (m);
$\lambda_i$	is the wavelength on Li (m);
$N_i$	is the integer phase ambiguity on Li (cycle);
$\phi_r(t_0, Li)$	is the initial phase of the receiver oscillator;
$\phi_s(t_0, Li)$	is the initial phase of the satellite oscillator;
$d_{mult/P(Li)}$	is the multipath effect in the measured pseudorange on Li (m);
$d_{mult/\Phi(Li)}$	is the multipath effect in the measured carrier phase on Li (m) and
$\varepsilon(.)$	is the measurement noise (m).

The non-zero initial phase  $\lambda_i(\phi_r(t_0, Li) - \lambda_i(\phi_s(t_0, Li)))$  in equation (2) is constant for an observed cycle-slip free satellite arc but differs for different satellites during an observation session. Less than one full cycle of the wavelength, this term is often merged into the integer ambiguity term  $\lambda_i N_i$ . In this case, equation (2) can be simplified as

$$\Phi(Li) = \rho + c(dt - dT) + d_{orb} + d_{trop} - d_{ion/Li} + \lambda_i N_i + d_{mult/\Phi(Li)} + \varepsilon(\Phi(Li)) \quad (3)$$

Note  $N_i$  ( $i = 1, 2$ ) in equation (3) is no longer an integer parameter. In [1], the following new observation system has been proposed:

$$P_{IF,Li} = 0.5(P(Li) + \Phi(Li)) \\ = \rho + c(dt - dT) + d_{orb} + d_{trop} + 0.5\lambda_i N_i + 0.5d_{mult/P(Li)} + 0.5\varepsilon(P(Li) + \Phi(Li)) \quad (4)$$

$$\Phi_{IF} = \frac{f_1^2 \cdot \Phi(L1) - f_2^2 \cdot \Phi(L2)}{f_1^2 - f_2^2} \\ = \rho + c(dt - dT) + d_{orb} + d_{trop} + \frac{cf_1 N_1 - cf_2 N_2}{f_1^2 - f_2^2} + d_{mult/\Phi(L1+L2)} \\ + \varepsilon(\Phi(L1 + L2)) \quad (5)$$

where  $i = 1, 2$ . Both combinations are ionosphere-free observations. Equation (5) is the traditional ionosphere-free phase observable, but equation (4) differs from the traditional

ionosphere-free code observation and its noise level is about half of the original code shown in equation (1). A combination of equations (4) and (5) provides an observation model system where both L1 and L2 ambiguities can be estimated so their integer characteristics can be exploited in PPP processing. As a result, fast ambiguity resolution algorithms can be developed to fix the ambiguities to their integer values and high precision positioning could be available with short initialization as required by real-time fast-static and kinematic applications. To further reduce the noise level of the new code combination as well as possible multipath effect, the well-known smoothing technique can be employed.

## PPP PROCESSING PROCEDURES

Since the ionosphere-free observation combination used for PPP processing in equation (4) and (5) are still affected by several other error sources including receiver and satellite clock error, orbital error and tropospheric error. For high precision point positioning, these errors should be eliminated or reduced to a negligible level. Precise GPS orbit and clock products are currently available from organizations contributing as Analysis Centers (AC) to the IGS and they can be applied for this purpose. Regarding the quality of the precise products, it is reported at an accuracy of 5 cm for the precise orbits and 0.2 nanoseconds for the precise clocks [2]. As to tropospheric delays, they can't be totally eliminated using the currently available troposphere models. Tropospheric delays consist of two types of delays: the dry part and the wet part as expressed in the following equation:

$$d_{\text{trop}} = d_{\text{dry}}^z \cdot f_{\text{map}} + d_{\text{wet}}^z \cdot f_{\text{map}} \quad (6)$$

where  $d_{\text{dry}}^z$  and  $d_{\text{wet}}^z$  denote the dry and wet zenith path delay respectively while  $f_{\text{map}}$  is a pre-defined mapping function. Usually about 90% of the tropospheric delays come from the dry component which can be estimated with a precision approaching 1% when pressure is known. The wet delay, however, is much more difficult to model and an error of 10-20% is common [4]. To reduce the influence of this error source, the wet trop zenith delay is modeled as an unknown parameter to be estimated together with other unknown parameters in the PPP processing.

Based on the new observation model suggested by Equations (4) and (5), PPP processing consists of the following unknown parameters in its estimator: a) three position coordinate parameters; 2) one receiver clock offset parameter; 3) one wet zenith tropospheric delay parameter and 4) L1/L2 ambiguity parameters equal to twice the number of visible satellites. Due to the existence of measurement noise and errors in precise orbit and clock products, their residual influence should be stochastically modeled in the parameter estimation process. Inappropriate stochastic information would not only degrade the estimation solution, but also provide false statistic results critical for data quality control and analysis. In order to ensure precise and reliable stochastic information, a stochastic estimation procedure has been developed and details can be found in [1].

## KINEMATIC ANALYSIS OF PPP PROCESSING

Numerical analysis was conducted using stationary GPS receivers at six stations and the

obtained results are presented in this section. The point positioning is carried out at a rate of 1Hz without applying any constraints on the receiver's motion and hence the positioning is conducted in a pure kinematic mode completely insensitive to the dynamics of the receivers.

## Data Description

Data used for the numerical computation were collected on August 15, 2001 from six Canadian Active Control Stations: DRA2, PRDS, YELL, CHUR, NRC1 and STJ0 (Figure 1). Dual-frequency receivers were used at all stations and the data-sampling rate was 1 Hz. The number of visible satellites was between 6 and 10 during the test period. The combined precise ephemeris in a SP3 format at a sampling interval of 15 minutes from IGS and the precise satellite clock corrections in a proprietary format at an interval of 30 seconds from NRCAN were used to eliminate the satellite orbital and clock errors. Since the observation data interval (1 second) was much shorter than the rate of precise GPS data, an interpolation technique based on Chebychev polynomials was applied to calculate the satellite's positions and clock corrections at each epoch. The unknown parameters to be estimated include three position coordinates, a receiver clock offset, a tropospheric wet zenith delay, and the ambiguity parameters of all visible satellites.



**Figure 1.** The six stations across Canada

## Results and Analysis

Figures 2 to 7 show the variations of position errors in latitude, longitude and height. The processing time in the unit of hour is shown in X-axis. All processing started at hour 0 but only the positioning results after the ambiguity estimates are converged (position RMS error is less than 40cm) are displayed.

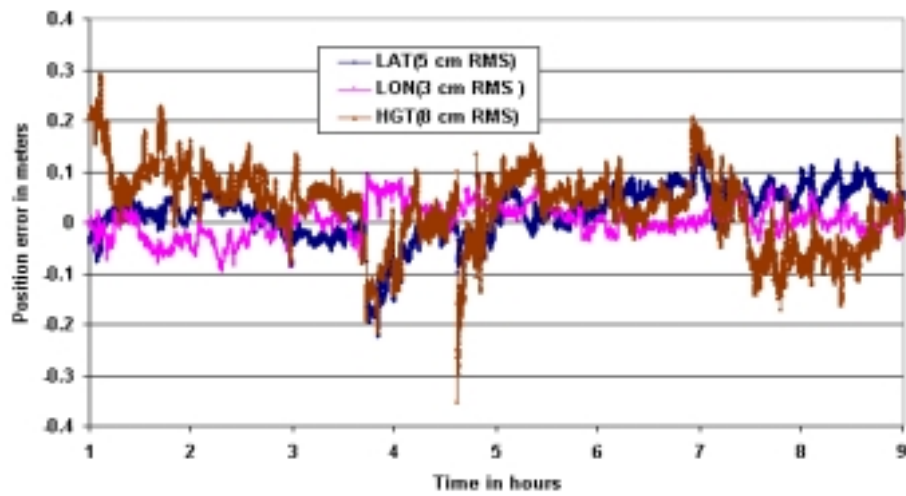


**Figure 2.** Kinematic results of nine hours of 1-Hz positioning of a static receiver at Station CHUR

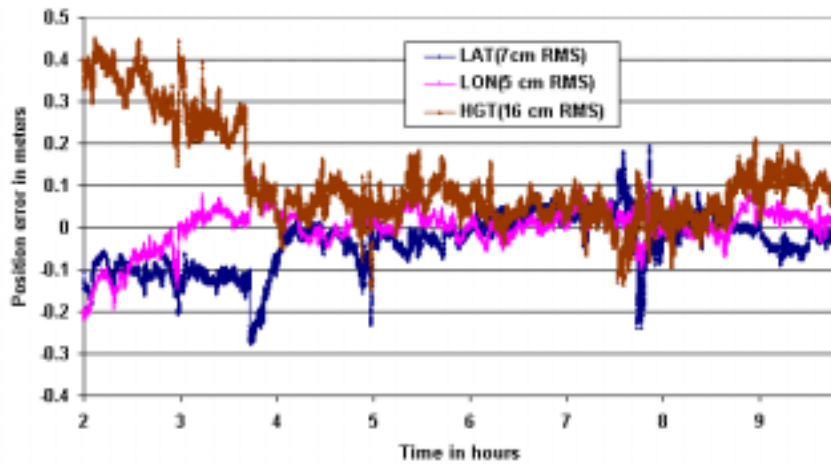


**Figure 3.** Kinematic results of ten hours of 1-Hz positioning of a static receiver at Station DRA2

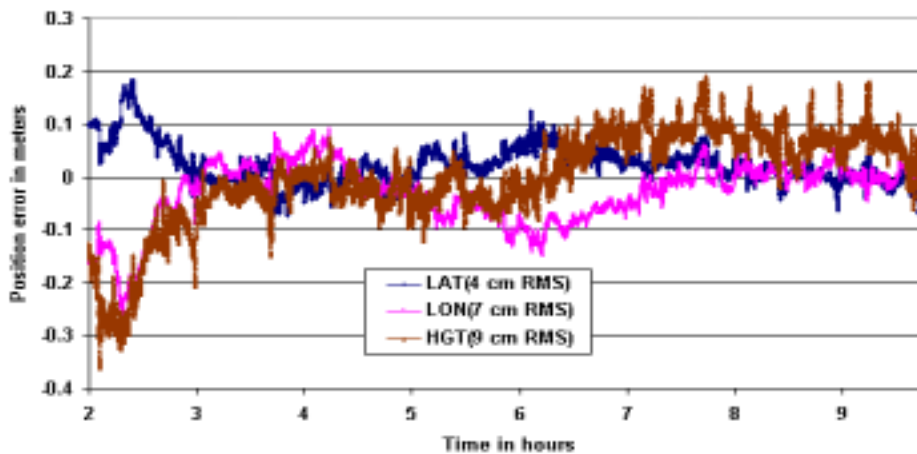


**Figure 4.** Kinematic results of ten hours of 1-Hz positioning of a static receiver at Station NRC1

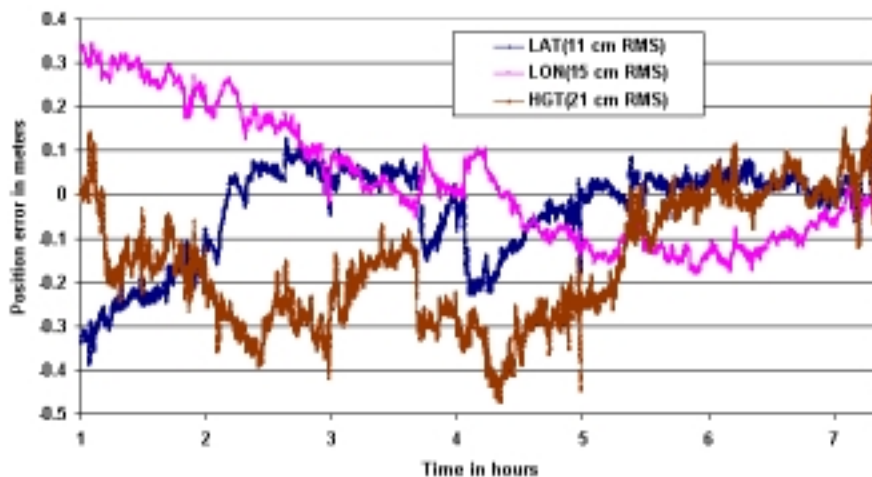


**Figure 5.** Kinematic results of eight hours of 1-Hz positioning of a static receiver at Station PRDS

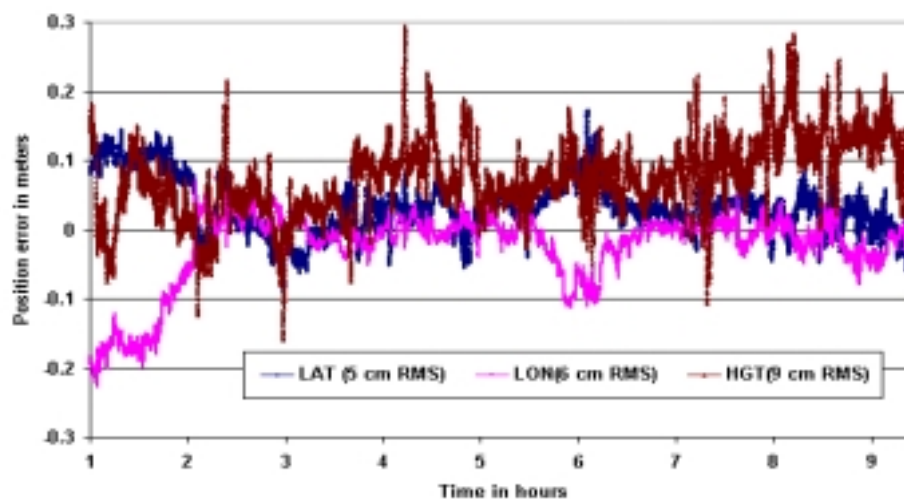


**Figure 6.** Kinematic results of ten hours of 1-Hz positioning of a static receiver at Station STJO

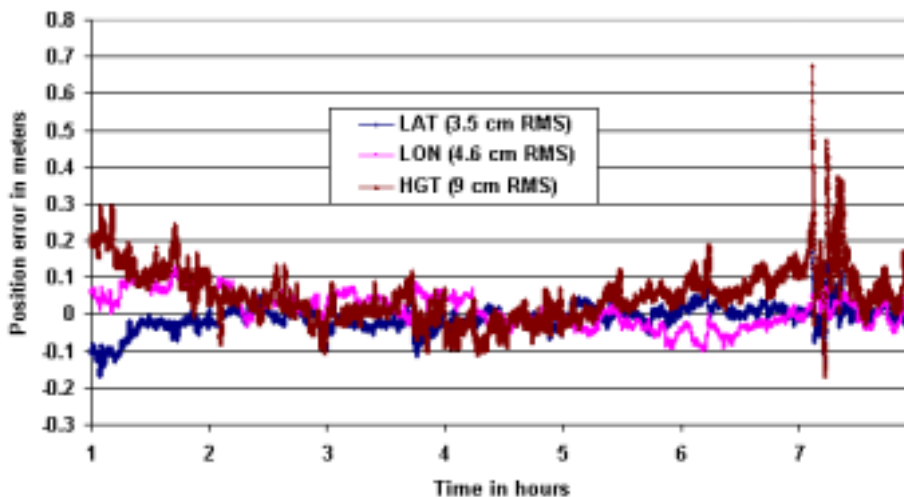


**Figure 7** Kinematic results of eight hours of 1-Hz positioning of a static receiver at Station YELL

The figures above display randomness of the position errors with a changing range of approximately 0.2 m centered at about zero value. For analyzing convenience, Table 1 lists the mean, sigma, and root mean square (RMS) values of the position errors in latitude, longitude, and height for all the above six processing results. We noticed the non-zero mean value at several centimetre level on the three directions for all stations. Table 2 summarizes the maximum, minimum and average RMS values for the six stations. An average of 12 cm vertical RMS error and less than 10 cm horizontal RMS error has been demonstrated.

**Table 1.** Statistics of kinematic processing accuracy

STATION		LAT (EAST)	LON (NORTH)	HEIGHT (VERTICAL)
CHUR (Average No. of Sat.: 7.7)	MEAN	0.019	0.004	0.030
	SIGMA	0.052	0.032	0.075
	RMS	0.055	0.032	0.081
DRA2 (Average No. of Sat.: 7.0)	MEAN	-0.036	-0.001	0.114
	SIGMA	0.065	0.050	0.114
	RMS	0.074	0.050	0.161
NRC1 (Average No. of Sat.: 6.8)	MEAN	0.023	-0.031	0.001
	SIGMA	0.038	0.06	0.091
	RMS	0.044	0.067	0.091
PRDS (Average No. of Sat.: 7.3)	MEAN	-0.038	0.029	-0.155
	SIGMA	0.107	0.146	0.140
	RMS	0.114	0.149	0.209
STJO (Average No. of Sat.: 7)	MEAN	0.033	-0.025	0.076
	SIGMA	0.040	0.054	0.055
	RMS	0.052	0.060	0.094
YELL (Average No. of Sat.: 8.2)	MEAN	-0.011	0.011	0.053
	SIGMA	0.033	0.045	0.072
	RMS	0.035	0.046	0.090

**Table 2.** Average RMS values of kinematic processing accuracy

RMS	East	North	Vertical
Maximum	0.114	0.149	0.209
Minimum	0.035	0.032	0.081
Average	0.062	0.067	0.121

In order to investigate what has caused the 12 cm vertical error and 10 cm horizontal error, provided in Table 3 are the mean converged position error under the kinematic processing mode, the corresponding RMS and sigma values, and the converged position error under the static processing mode. Results from Station CHUR are studied, and 6 four-hour samples from a 24-hour continuous dataset were processed in a static way. Since the results have demonstrated similarities among the converged position errors from the 6 four-hour static processing samples, a conclusion can be made that the non-zero kinematic mean position errors and the converged static position error mostly comes from the systematic error such as

the error in our used known coordinates. On the other hand, the 10 cm RMS position error with a PDOP of 0.7 is quite conformable to the residual error of the precise ephemeris (3~5 cm RMS) and clock correction (0.1~0.2 nanosecond RMS, or 3~6 cm) [2].

**Table 3.** Statistics of static and kinematic positioning accuracy at Station CHUR

	<b>EAST (LAT)</b>	<b>NORTH (LON)</b>	<b>VERTICAL (HEIGHT)</b>
Static Positioning error	0.023	-0.002	0.050
Mean (kinematic)	0.019	0.004	0.030
RMS (kinematic)	0.055	0.032	0.081
SIGMA (kinematic)	0.052	0.032	0.075

As to the time required for the float position solution to converge, Figure 8 shows the kinematic position error of nine hours of 1-Hz positioning of a static receiver at station CHUR. Approximately 50 minutes is needed for the position estimation to reach convergence in this case. If all six stations are considered, an average of about 2 hours is required for the position estimation to converge to 1~2 decimetre in the kinematic mode.

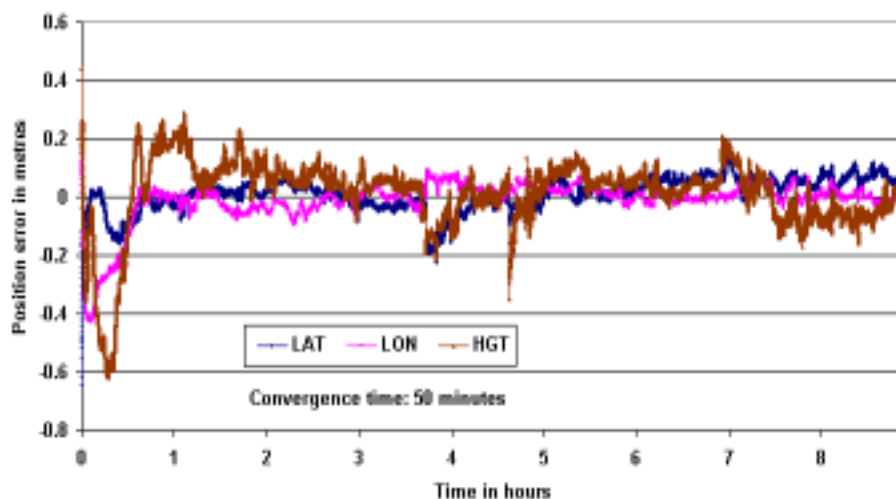


**Figure 8.** Kinematic position error in nine hours of 1-Hz positioning of a static receiver at Station CHUR, and its time of convergence

Tropospheric effect is also studied, which is showed in Figure 9 below. TROP-S represents the static results which act as the true tropospheric effects, while TROP-K for the kinematic. A nine-hour processing at Station CHUR shows an agreement at 4mm RMS level.

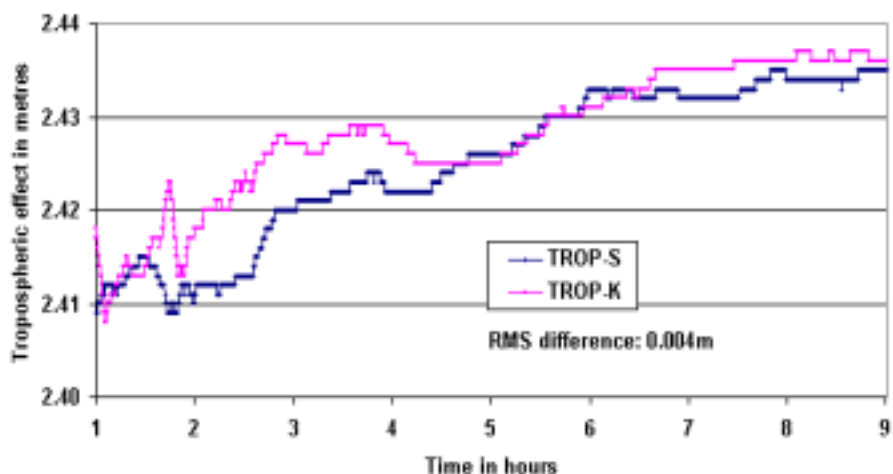


**Figure 9.** Kinematic processing estimate of tropospheric effect at a stationary site compared against static processing results at Station CHUR

## CONCLUSION

Kinematic positioning analysis of a carrier phase-based precise point positioning system has been presented in this paper. The numerical analysis has been conducted using data from six permanent GPS tracking stations. The kinematic positioning results have shown an average RMS value of 12 cm vertical positioning error and less than 10 cm horizontal positioning error. An average of 2 hours is needed for position to converge to an accuracy of a few centimetres indicating the importance for the development of integer ambiguity fixing methods for PPP processing.

## ACKNOWLEDGEMENTS

This research is partially supported by a NSERC grant and a GEOIDE grant held by the second author. Contribution of data and consultation with personnel from Natural Resources Canada, Geodetic Survey Division is also appreciated.

## REFERENCES

- [1] Gao, Y. and Shen, X. (2001). "Improving Ambiguity Convergence in Carrier Phase-Based Precise Point Positioning", Proceedings of ION GPS-2001, Salt Lake City, .
- [2] Kouba, J And Heroux, P. (2000). "Precise Point Positioning Using IGS Orbit Products", GPS Solutions, Vol.5, No.2, Fall, pp12-28.
- [3] Muellerschoen, R.J. Y.E. Bar-Sever, W.I. Bertiger, D.A. Stowers (2001). "NASA's Global DGPS for High Precision Users", GPS World, Vol. 12, No. 1, pp.14-20.
- [4] Rizos, C. (2000). *Principles and Practice of GPS Surveying*, University of New South Wales.
- [5] Teunissen, P.J.G. and A. Kleusberg (Eds.) (1998). *GPS for Geodesy*, Second Edition,

Springer-Verlag, New York.

- [6] Zumberge, J.F., Heflin, M.B., Jefferson, D.C., Watkins, M.M., & Webb, F.H. (1997). "Precise Point Positioning for the Efficient and Robust Analysis of GPS Data from Large Networks". *J. Geophys. Res.*, 102, pp. 5005-5017.

## **BIOGRAPHICAL NOTES**

**Dr. Yang Gao** is an Associate Professor in the Department of Geomatics Engineering at the University of Calgary. He currently leads a project to develop methods and algorithms to support real-time precise point positioning. **X. Shen** is an Msc student in the same department.